IEEE Access
Multidisciplinary | Rapid Review | Open Access Journal

Packet Level Performance Assessment of mmWave Backhauling Technology for 3GPP NR Systems

ALEKSANDR OMETOV, (Member, IEEE), DMITRI MOLTCHANOV, MIKHAIL KOMAROV, (Senior Member, IEEE), SERGEY VOLVENKO, YEVGENI KOUCHERYAVY (Senior Member, IEEE)

Corresponding author: D. Moltchanov (e-mail: dmitri.moltchanov@tut.fi).

ABSTRACT Recently standardized millimeter-wave (mmWave) band 3GPP New Radio systems are expected to bring extraordinary rates to the air interface efficiently providing commercial-grade enhanced mobile broadband services in hotspot areas. One of the challenges of such systems is efficient offloading of the data from access points (AP) to the network infrastructure. This task is of special importance for APs installed in remote areas with no transport network available. In this paper, we assess the packet level performance of mmWave technology for cost-efficient backhauling of remote 3GPP NR APs connectivity "islands". Using a queuing system with arrival processes of the same priority competing for transmission resources, we assess aggregated and per-AP packet loss probability as a function environmental conditions, mmWave system specifics and generated traffic volume. We show that the autocorrelation in aggregated traffic provides a significant impact on service characteristics of mmWave backhaul and needs to be compensated by increasing either emitted power or the number of antenna array elements. The effect of autocorrelation in the per-AP traffic and background traffic from other APs also negatively affects the per-AP packet loss probability. However, the effect is of different magnitude and heavily depends on the load fraction of per-AP traffic in the aggregated traffic stream. The developed model can be used to parameterize mmWave backhaul links as a function of the propagation environment, system design, and traffic conditions.

I. INTRODUCTION AND MOTIVATION

Today, the development of wireless systems and uncontrollable growth of the interconnected devices number pushed the community towards developing new technology which is expected to provide support for the demands of tomorrow outlined by IMT-2020. One of the technology enablers that recently came to the research community attention is 5G New Radio (5G NR) based on mmWave technology [1].

The primary goal of 5G NR is to reach the performance characteristics of fiber-like links in wireless domain [2]. 5G NR was standardized by 3GPP Rel. 15 in December 2017 and is expected to be on the chipset market soon [3]. The non-standalone architecture leverages the LTE and 5G NR air interfaces as well as the existing LTE core network. This configuration will likely be used for early 2019 deployments [4]. Enabling such high throughput at the last mile of the network leads to higher load at the intermediate communication links. The fiber optic technology currently utilized for connecting BSs to the infrastructure could handle this load in most of the situations [5], [6]. However, there are scenarios, where BS connectivity via fiber is not feasible, for example, islands or ski resorts. In those cases, network operators are forced to rely on wireless backhaul links with highly directional antennas [7]. 3GPP standardization activities are in progress attempting to address the requirements and challenges of wireless backhaul links that utilize mmWave and higher frequency band. Notably, the Integrated Access Backhaul (IAB) is expected to provide improved topology management, better route optimization, and higher spectral efficiency together with better reliability [8].

Conventionally, the performance of the backhauling technology is studied using the tools of stochastic geometry. These models capture channel variations induced by random locations of communicating entities often taking simplified

assumptions about traffic load. When two or more traffic flows from remote NR APs are aggregated over the backhaul link, properties of individual flows, as well as dependencies, be- tween them may drastically affect backhaul performance. In this paper, aiming at characterizing mmWave backhaul parameters including the dedicated bandwidth, emitted power, antenna configurations at both sides of a communications link in complex weather and traffic conditions, we develop a packet level performance evaluation model. The system of interest is modeled by a queuing system with multiple autocorrelated concurrent processes of the same priority competing for transmission resources. The service time follows generic distribution and is related to mmWave propagation specifics. We analytically characterize losses experienced by both individual flow and aggregated traffic as a function of system parameters.

The main contributions of our study are:

- Queuing-theoretic packet level performance evaluation model capturing specifics of mmWave system design and channel propagation in different environmental conditions and allowing to investigate aggregated and per-AP performance metrics of interest;
- Numerical assessment of systems and channel parameters allowing to maintain the prescribed values of per-AP and aggregated traffic packet loss probabilities;
- Numerical assessment of the effect of autocorrelation in the per-AP and aggregated traffic flows showing that it negatively affects the associated packet loss probabilities and needs to be compensated by the improved channel capacity by increasing either emitted power or the number of antenna array elements forming the radiation or sensitivity patterns.

The rest of the paper is organized as follows. First, we cover the related work on mmWave backhauling and the queuing models with multiple arrival flows in Section II. Further, we describe the scenario of interest in Section III. In Section IV, we develop the performance evaluation framework. Numerical assessment is carried out in Section V. The conclusions are drawn in the last section.

II. RELATED WORK

A. MMWAVE BACKHAULING

The efficient use of by 5G NR systems naturally calls for cost-efficient wireless backhauling matching the rates offered at the air interface. The use of mmWave spectrum is thus considered as a logical choice for 5G backhauls. The fundamental study in [9] elaborates on the general evolutionary movement towards backhauling in 5G that would enable wide-area Gbps coverage. Similarly, the authors in [10] bring readers attention to redesigning wireless relayed backhauls by jointly optimizing their topology, power, and bandwidth utilization. Authors in [11] discuss the applicability of mmWave backhauling for small cell heterogeneous networks and related challenges [12] highlighting the benefits of using massive MIMO antenna arrays with high receptivity. The study in [13] further proposes scheduling mechanisms to improve energy efficiency by optimizing simultaneous transmission scheduling and power control for the mmWave backhauling. The industry-driven analysis in [14] elaborates on the eligibility of self-backhauling as a solution for a simple cost-efficient strategy to enable dense mmWave cellular networks. The authors in [15], [16] propose to use terahertz (THz) frequencies for the 5G NR backhauling. However, the requirement for line-of-sight (LoS) operation and inherent high atmospheric attenuation makes long-distance backhauling in the THz band a challenging task.

Backhaul links are also expected to aggregate traffic streams from a number of APs into a single bundle for further transmission over the wireless medium. Most of the papers published so far concentrated on principle feasibility mmWave/THz backhaul designs neglecting the properties of aggregated traffic streams from multiple NR APs. At the same time, the choice of the bandwidth, antenna configurations, and other long-distance mmWave link parameters heavily depend on the traffic generated users associated with APs. The choice of the optimal operational parameters of mmWave backhauls (bandwidth, antenna configurations, etc.) is critical as the same spectrum is shared between user and backhaul interfaces. Furthermore, since these traffic streams can be heterogeneous in nature and may have different service requirements, the decision on the optimal parameters may depend on individual flow performance. Per-source analysis of heterogeneous sources is non-trivial as the contribution of each multiplexed source needs to be explicitly accounted. It becomes even more challenging when individual flows are autocorrelated as it usually happens in practice.

B. QUEUING SYSTEMS WITH CONCURRENT FLOWS

Performance parameters provided to the single traffic flow in the presence of a certain number of concurrent flows of the same priority have not been deeply studied so far. In [17], Beritelli *et al*. consider a packet multiplexor loaded with a number of voice-over-IP (VoIP) streams each of which was modeled using a special case of discrete-time batch Markovian arrival process (D-BMAP). The service time was assumed to be constant and equal to the time unit. Performance parameters of interest were the mean number of lost packets and the mean delay of a packet experienced by individual sources. Unfortunately, only quantitative results were provided by the authors. A similar model with infinite buffer has been studied in [18]. Using generating functions approach, the authors obtained the mean delay experienced by packets emitted by a single source. The extended model of the general case of $\sum$D-BMAP/D/1/K queuing system is given in in [19]. The authors obtained expressions for probability mass function (pmf) of the number of lost packets in a slot and delay of an arbitrary packet from a single source.

Fiems *et al*. [20] considered the model with two Markov modulated arrival sources and generally distributed service times. Performance parameters of interest were the packet loss probability, consecutive packet loss probability, and

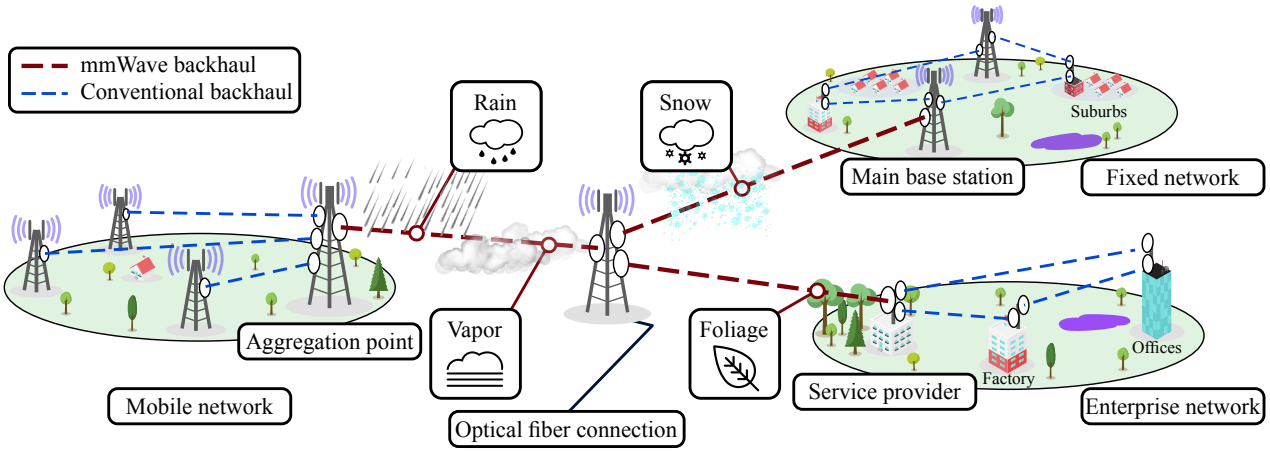

FIGURE 1. Illustration of the considered mmWave backhaul scenario for 3GPP NR systems.

moments of the number of successfully accepted packets from a single source between two consecutive losses. Unfortunately, no results for distribution functions of these metrics have been provided. Finally, MMPP+MMPP/E_r/1/K and MMPP+M/M/1/K models have been analyzed in [21], [22]. Motivated by applications of forward error correction (FEC) the authors obtained per-source packet loss characteristics including the packet loss probability and the probability that there are exactly k losses in a sequence of n packets.

III. SYSTEM MODEL

In this section, we define the system model by introducing its components including the deployment of interest, propagation model under different environmental conditions, antenna and traffic models, as well as our metrics of interest. Main notations used in this work are given in Table 1.

A. DEPLOYMENT CONSIDERATIONS

Overall, we consider a scenario with a number of edge access points (including base stations and local service provider APs) serving the area of interest. The APs' traffic collected from the conventional users tends to get aggregated at just one link at some point. The system model of the backhaul link we use in our study is shown in Fig. 1. This brings us to the conventional problem of the backhaul bottleneck. In our case, this link is a mmWave backhaul connecting the APs with the optical fiber that, in turn, provides higher capacity access to the global network. We assume that a certain number of flows of the same priority, that may themselves be traffic aggregates, share a wireless link of the constant bit rate raw capacity. We assume that the size of all packets is constant and equal to L bytes including all headers. The buffering is done at the IP layer. The number of waiting positions in the buffer is limited to $(K-1)$ packets. Whenever there is at least one packet in the buffer, and the channel is free for transmission – this packet is scheduled to the data-link layer.

Although specific standards for mmWave backhaul links are to be specified within the next two years by 3GPP, they are expected to inherit most of 3GPP NR functionality. We assume that data-link and physical layers functionality including the set of modulation and coding schemes (MCS) to follow 3GPP NR as described in [23].

B. PROPAGATION MODEL

The signal-to-noise ratio (SNR) in the linear scale at the receiver located at a distance x from the AP is $S(x) = (P_T G_T G_R)/(JBL(x))$, where P_T is the transmit power, G_T and G_R are the antenna gains at the transmitter and receiver sides, respectively, which depend on the antenna array, $L(x)$ is the path loss in linear scale, J is the Johnson-Nyquist noise at one Hz, B is the operational bandwidth.

Following 3GPP the path loss measured in dB is [24]

$$L_{dB}(x) = 32.4 + 21\log(x) + 20\log f_c, \qquad (1)$$

where f_c is operational frequency measured in GHz, and x is the distance between AP and UE. We note that the effect of LoS blockage that is detrimental to 3GPP NR access links is not expected to play an important role in backhauls dimensioning. The reason is that in most cases there is a way to install transceivers at a certain height such that LoS between two ends of a link is available.

Being specified for access technologies, the previous model does not include two important characteristics inherent for long-distance backhaul links. Overall, the backhaul link operating at mmWave or higher frequencies could be affected by the weather conditions [25]. Several studies so far reported on measurements on mmWave propagation conditions under various meteorological impairments [26], see Table 2. Note, that the most significant impact is produced by foliage, up to 2 dB/m. The impairments brought by heavy snow and fog/clouds are fairly insignificant (less than 1 dB/km) for realistic backhaul distances. On the other hand, rain is typically characterized by around 10 dB/km of additional attenuation

TABLE 1. Notation used in the paper.

Notation	Details
$S(x)$	SNR at the receiver located at a distance x
P_T	The transmit power
G_T, G_R	The antenna gains at the transmitter and receiver
$L(x)$	The path at the receiver located at a distance x
J	The Johnson-Nyquist noise
α_T, α_R	HPBW angles of the radiation pattern
θ_{3db}	The 3-dB point of the radiation pattern
β	Antenna array direction angle
N	Number of antenna elements
Δt	Slot duration
D	The transition probability matrix of D-BMAP
M	Number Markov modulating chain states of D-BMAP
$W(n)$	Discrete-time batch Markovian arrival process
$Y(n)$	Modulating Markov chain of D-BMAP process
$\vec{\pi}$	The steady-state vector of the modulating Markov chain
A, B, T	Indices for aggregated, tagged and background processes
$\vec{E}$	The mean vector of D-BMAP
ϵ_l	The ls eigenvalue of D
$\vec{g}_l, \vec{h}_l$	ls left and right eigenvectors of D
$\vec{e}$	The vector of ones
L	Packet size in bytes
K	The capacity of the system measured in IP packets
$Y_Q(n)$	The number of packets in the system
$Z(i,j)$	Blocks of transition probability matrix of the queue
T	Transition probability matrix of the queuing model
$\vec{x}_D, \vec{x}$	Steady-state distribution at the departure and arbitrary slots
L_A, L_T	Number of lost packets from aggregated and tagged flows
$I_L(n)$	The indicator of the event that at least one packet is lost
C_i^n	Combination of i elements from n
$\psi(\cdot)$	Probability of arrangement of packets from tagged source
$I_L(n)$	The indicator of the loss event in the slot n
R_A, R_T	Arrival rates from aggregated/tagged flows
ρ_A, ρ_T	Offered load from aggregated/tagged flows
$K_{A,0}, K_{T,0}$	Lag-1 NACFs of aggregated/tagged flows

that may severely affect backhaul performance.

Based on the considerations listed above, in this paper we address impairments caused by rain. To account for 10 dB/km degradation we modified the 3GPP propagation model to take the following form $L_{dB}(x) = 32.4 + 24.5\log(x) + 20\log f_c$.

In addition to weather conditions, the transmission is also affected by atmospheric absorption. These impairments heavily depend on the operational frequency and drastically vary as illustrated in Fig. 2. In the frequency range $30 - 100$ GHz the most impact is provided by oxygen and water vapor. Accounting for absorption, the overall losses at 28 GHz is

$$L_dB(x) = \begin{cases} 32.4 + 29.5\log(x) + 20\log f_c, & \text{clear}, \\ 32.4 + 33.1\log(x) + 20\log f_c, & \text{rain}. \end{cases} \quad (2)$$

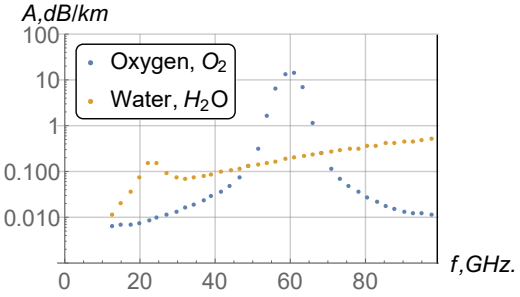

FIGURE 2. Absorption losses caused by various atmospheric substances.

C. ANTENNA ARRAYS

Following [35], we assume linear antenna arrays at both the transmit and receive sides. The crucial coefficients of the antenna model – the transmit and receive directivities α_T and α_R – need to be related to the parameters of the antenna arrays. Half-power beamwidth (HPBW) of the array, α, is proportional to the number of elements in the appropriate plane and is $\alpha = 2|\theta_m - \theta_{3db}|$, where θ_{3db} is the 3-dB point and θ_m is the location of the array maximum [36]. The latter is $\theta_m = \arccos(-\beta/\pi)$, where β is the array direction angle.

Assuming $\beta = 0$, we have $\theta_m = \pi/2$. The upper and lower 3-dB points are thus $\theta_{3db}^{\pm} = \arccos[-\beta \pm 2.782/(N\pi)]$, where N is the number of antenna elements. For $\beta = 0$, the mean antenna gain over HPBW is [36]

$$G = \frac{1}{\theta_{3db}^{+} - \theta_{3db}^{-}} \int_{\theta_{3db}^{-}}^{\theta_{3db}^{+}} \frac{\sin(N\pi\cos(\theta)/2)}{\sin(\pi\cos(\theta)/2)} d\theta. \quad (3)$$

D. TRAFFIC MODELS

We model the packet arrival processes using D-BMAP. General D-BMAP is defined as follows. Assume the discrete-time environment, i.e., time axis is slotted, the slot duration is constant and given by Δt. Consider the discrete-time homogeneous ergodic Markov chain $\{Y(n), n = 0, 1, \dots\}$ defined at the state space $Y(n) \in \{1, 2, \dots, M\}$. Let D be its transition probability matrix and $\vec{\pi} = (\pi_1, \pi_2, .., \pi_M)$ be the row array containing equilibrium state probabilities. Let then $\{W(n), n = 0, 1, ..\}$ be a D-BMAP whose underlying Markov chain is $\{Y(n), n = 0, 1, \dots\}$. We define D-BMAP as the set of matrices $D(k)$, $k = 0, 1, \dots$, each containg of transition probabilities with $k = 0, 1, \dots$, arrivals, respectively. It is easy to see that for each pair of states $i, j \in \{1, 2, \dots, M\}$ the following elements of $D(k)$

$$d_{ij}(k) = Pr\{W(n) = k, Y(n) = j | Y(n-1) = i\}, \quad (4)$$

are conditional pmfs of D-BMAP.

Let $\vec{E} = (E_1, E_2, \dots, E_M)$ be the mean vector of D-BMAP, where $E_i = \sum_{j=1}^{M} \sum_{k=1}^{\infty} k d_{ij}(k)$, $i = 1, 2, \dots, M$.

TABLE 2. Environmental effects on mmWave propagation losses

Type	Reference	Scenario	Measurements
Rain	[27]–[29]	Rate of 50 mm/hr	<10 GHz: $1-6$ dB/km >10 GHz: 10 dB/km
Fog/cloud	[30], [31]	Density of 0.5g/m^3	50.44 GHz: 0.16 dB/km 81.84 GHz: 0.349 dB/km
Snow	[32]	Density of 700g/m^3	$35-135$ Ghz: $0.2-1$ dB/km
Foliage	[33], [34]	Density of 0.5m^2/m^3	28.8, 57.6 GHz: $1.3-2.0$ dB/m 73 GHz: 0.4 dB/m

The ACF of the mean process of D-BMAP is [37]

$$R_E(i) = \sum_{l,l\neq 1} \phi_l \epsilon_l^{i-1},\ i = 1, 2, \ldots,$$
$$\phi_l = \vec{\pi} \sum_{k=0}^{\infty} kD(k)\vec{g}_l \vec{h}_l \sum_{k=0}^{\infty} kD(k)\vec{e}, \tag{5}$$

where ϵ_l is the ls eigenvalue of D, $\vec{g}_l$ and $\vec{h}_l$ are ls left and right eigenvectors of D, and $\vec{e}$ is the vector of ones.

In this paper, we define two arrival processes. These are the tagged process, $\{W_T(n), n = 0, 1, \ldots\}$, representing superposed traffic from a randomly selected AP and the background process, $\{W_B(n), n = 0, 1, \ldots\}$, modeling superposed traffic from the rest of APs. As D-BMAP is closed with respect to the superposition property, the background process can represent the superposition of arrivals from a number of APs.We denote superposition of the tagged and background arrival processes as $\{W_A(n), n = 0, 1, \ldots\}$, where subscript A stands for aggregation. Let $D_T(k)$, $D_B(k)$, $D_A(k)$, $k = 0, 1, \ldots$ be the transition probability matrices with exactly k arrivals of corresponding processes. Then, transition probability matrices with k, $k = 0, 1, \ldots$ arrivals from the aggregated process can be found using Cartesian product of the transition probability matrices of individual processes as

$$D_A(k) = \sum_{i=0}^{k} D_T(i) \otimes D_B(k-i),\ k = 0, 1, \ldots \tag{6}$$

In what follows, we will also need transition probability matrices of the superposed process with exactly i, $i = 0, 1, \ldots$, arrivals from the tagged process and j, $j = 0, 1, \ldots$, arrivals from the background process. We denote them as $D_A(i, j)$, $i = 0, 1, \ldots$, and derive as follows

$$D_A(i, j) = D_T(i) \otimes D_B(j). \tag{7}$$

E. METRICS OF INTEREST

The metrics of interest are those related to aggregated and per-source traffic performance over the mmWave backhaul. Thus, we concentrate on the pmfs of the number of lost packets from both aggregated and per-source traffic streams.

IV. PERFORMANCE EVALUATION FRAMEWORK

In this section, we present our performance evaluation framework. We start by describing our modeling methodology. Then, we introduce the queuing model and its solution for stationary-state probabilities. Finally, we characterize aggregate and per-source packet loss probabilities.

A. MODELING METHODOLOGY

The packet losses in mmWave wireless backhauls can happen due to both imperfect error concealment at the air interface, and buffer overflows. In our study, we decompose the complex problem of modeling performance of packet transmission over mmWave backhaul link to two simpler problems: (i) characterization of the effective rate provided by the backhaul link and (ii) analysis of queuing performance. This decomposition is feasible due to the use of adaptive modulation and coding schemes (MCS) at the air interface in modern cellular technologies including mmWave systems [23]. In particular, there is always an MCS specifying the effective rate of the mmWave backhaul and bounding packet losses by a given value for given environmental conditions. Using the effective rate, we proceed to specify a queuing model and characterize the aggregated and per-source packet losses caused by buffer overflows.

B. QUEUING MODEL

To account for two specified arrival processes, we model the buffering process at the mmWave backhaul using the D-BMAP$_T$+D-BMAP$_B$/G/1/K, where K is the capacity of the system measured in IP packets. System time is discrete with constant slot duration Δt given by the time required to transmit one IP packet. The first step in the analysis is to find the steady-state distribution of the number of packets in the system at the arbitrary time slot and just before the arrival of a batch. To achieve that, we consider D-BMAP$_A$/D/1/K queuing system, where the arrival process is the superposition of $\{W_T(n), n = 0, 1, \ldots\}$ and $\{W_B(n), n = 0, 1, \ldots\}$.

Time diagram of D-BMAP$_A$/G/1/K queuing system is shown in Fig. 3. According to this system, packets arrive in batches just before the end of slots. Arrivals are not allowed to seize the server immediately, and the service of any arrival starts at the beginning of a slot. Packets depart from the system at the slot boundaries, just after batch arrivals.

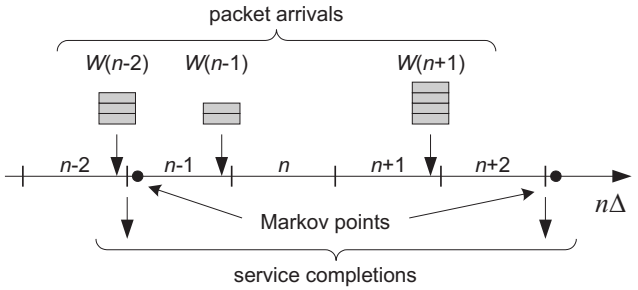

FIGURE 3. Time diagram of D-BMAP$_A$/G/1/K queuing system.

The state of the system is observed just after departure. This system is known as the late arrival model with delayed access [38], [39]. We assume partial batch acceptance strategy.

The complete description of the queuing system requires two-dimensional Markov chain $\{Y_Q(n), Y_A(n), n = 0, 1, \dots\}$ imbedded at the moments of packet departures from the system, where $Y_A(n) = Y_B(n) \otimes Y_T(n)$ is the state-space of the aggregated arrival process, $Y_Q(n) \in \{0, 1, \dots, K-1\}$ is the number of packets in the system just after packet departures.

Let $D_A(i,k)$, $k = 0, 1, \dots$, $i = 0, 1, \dots$, be the set of matrices containing i-steps transition probabilities of the modulating Markov chain of the arrival process with exactly k packet arrivals. Setting $D_A(1,k) = D_A(k)$, $k = 0, 1, \dots$ we find them using $D_A(k)$, $k = 0, 1, \dots$, as follows

$$D_A(i,k) = \sum_{l=0}^{i} D_A(l, k-1) D_A(i-l). \tag{8}$$

Let $D_Q(k)$, $k = 0, 1, \dots$, be the set of matrices describing transitions from the state i to the state j, i.e., $i, j \in \{0, 1, \dots, M\}$ of the modulating Markov chain of the arrival process with exactly k arrivals in a service time of a single packet. We determine them using the service time distribution, $d(k)$, $k = v, v+1, \dots, r$ as

$$D_Q(k) = \sum_{i=0}^{\infty} D_A(k,i) d(i), \qquad k = 0, 1, \dots \tag{9}$$

Let $Z(i,j)$, $i, j \in \{0, 1, \dots, K\}$ be transition probability matrices describing time evolution of the $\{Y_Q(n), Y(n), n = 0, 1, \dots\}$. These matrices can be completely defined using $D_Q(k)$, $k = 0, 1, \dots$ as follows

$$Z(0,j) = \begin{cases} D_Q(k), & j \neq K, \\ \sum_{m=K}^{\infty} D_Q(m), & j = K, \end{cases}$$
$$Z(i,j) = \begin{cases} D_Q(j-i+1), & j \neq K,\ j > i-2, \\ \sum_{m=K-i}^{\infty} D_Q(m), & j = K,\ j > i-2. \end{cases} \tag{10}$$

Let T be transition probability matrix containing $Z(i,j)$, $i, j \in \{1, 2, \dots, M\}$ as its (i,j) elements and let $\vec{x}_D = (x_{D,01}, .., x_{D,K-1M})$ be its steady-state distribution. Solving $\vec{x}_D T = \vec{x}_D$, $\vec{x}_D \vec{e} = 1$, we get $x_{D,kj} = Pr\{Y_Q(n) = k, Y(n) = j\}$. There are a number of numerical algorithms to compute $\vec{x}_D$, e.g., [40]–[42].

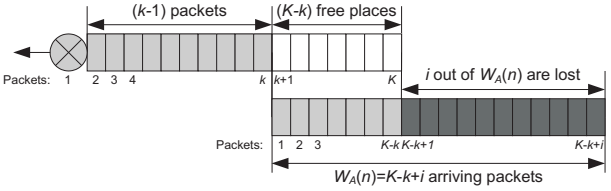

FIGURE 4. Case when i out of $W_A(n)$ packets are lost in the slot n.

To obtain pmfs of the number of lost packets in a slot we need steady-state probabilities of the number of packets in the system in the arbitrary slot. Using the flow balance principle, it was shown that for the D-BMAP/G/1/K late arrival system the following relation between steady-state probabilities at departure, $\vec{x}_D$, and arbitrary time slot, $\vec{x}$, holds [43]

$$\left[\vec{\pi}_A \sum_{k=0}^{\infty} D_A(k) \vec{e}\right] \vec{x}_{D,i} = \vec{x}_i (D_A - D_A(0)). \tag{11}$$

C. LOSS PERFORMANCE OF THE AGGREGATED FLOW

Consider first loss performance of the aggregated flow. We characterize it by obtaining pmf of the number of lost packets in a single slot. Let the RV L_A, $L_A \in \{0, 1, \dots\}$, denote the number of lost packets in a slot and let $f_{L_A}(i) = Pr\{L_A(n) = i | W_A(n) \geq 1\}$, $i = 0, 1, \dots$, be its pmf conditioned on the event of at least one packet arrival from the aggregated arrival process.

Consider the case when exactly i, $i = 1, 2, \dots$, packets are lost in the slot n. It happens when the following conditions are simultaneously met, see Fig. 4, (i) there are exactly k, $k = 0, 1, \dots, K$ packets in the system in the slot $(n-1)$ and (ii) the number of arriving packets in the slot n is exactly $K - k + i$. We have

$$f_{L_A}(i) = \frac{\sum_{k=0}^{K} \vec{x}_k D_A(K-k+i) \vec{e}}{Pr\{W_A(n) \geq 1\}}, \ i = 1, 2, \dots, \tag{12}$$

where $\vec{e}$ is the vector of ones of appropriate size, $\vec{x}_k$, $k = 0, 1, \dots, K$ is the vector containing steady-state probabilities that there are exactly k packets in the system in an arbitrary slot. Observe that $f_{L_A}(0)$ can be obtained as $1 - \sum_{i=1}^{\infty} f_{L_A}(i)$

The probability of at least one packet arrival is

$$Pr\{W_A(n) \geq 1\} = \vec{\pi}_A \sum_{i=1}^{\infty} D_A(i) \vec{e}, \tag{13}$$

where $\vec{\pi}_A$ is the steady-state probability vector.

We get $f_{L_A}(i)$, $i = 0, 1, \dots$ by substituting (13) in (12).

D. PER-SOURCE LOSS PERFORMANCE

Now, we proceed deriving expression for pmfs of the number of lost packets arriving in a slot from the tagged arrival process. Here, in addition to characterizing the number of lost packets we also need to specify which of those actually belong to the tagged process.

Consider behavior of D-BMAP$_B$+D-BMAP$_T$/G/1/K system between two arbitrary imbedded Markov points. Since the number of arrivals per slot from both process is virtually unlimited, there can be infinitely many lost packets in a slot. Let the RV L_T, $L_T \in \{0, 1, \dots\}$, denote the number of lost packets in a slot and let $f_{L_T}(j) = Pr\{L_T(n) = j | W_T(n) \geq 1\}$, $j = 0, 1, \dots$, be its pmf conditioned on the event of at least one packet arrival from the tagged source.

Firstly, consider the case when $L_T = 0$, i.e., the tagged arrival process does not lose any packets. Here, we have to find the probability that the system successfully accommodates all the arriving packets from the tagged source. Observe that the tagged source may not lose any packets even when $W_B(n) + W_T(n) \geq K - k$, i.e., when the number of arrivals from both processes is greater than the system can accommodate. However, at least one arrival form the tagged source is always lost when $W_T(n) > K - k$. We consider $f_{L_T}(0)$ as a sum of two components. The first component corresponds to the case when the tagged process cannot lose a packet in a slot, i.e., $W_B(n) + W_T(n) \leq K - k$. The second one – to the case when some packets arriving from the tagged source can be lost, i.e., $W_B(n) + W_T(n) > K - k$.

Let $I_L(n)$ be the indicator of the event that at least one packet loss in the slot n from the aggregated process. For i, $i = 0, 1, \dots$, lost packets in a slot we define the following conditional pmfs

$$f_{L_T}(i, j) = Pr\{L_T(n) = i, I_L(n) = j | W_T(n) \geq 1\}. \quad (14)$$

Using (14), we have

$$f_{L_T}(i) = f_{L_T}(i, 0) + f_{L_T}(i, 1),\ i = 0, 1, \dots \quad (15)$$

Consider case when $W_B(n) + W_T(n) \leq K - k$, i.e., the tagged source cannot lose a packet and let us firstly concentrate on obtaining $f_{L_T}(0)$. Observe that $f_{L_T}(i, 0) = 0$, $i = 1, 2, \dots$ meaning that only $f_{L_T}(i, 0)$ contributes to $f_{L_T}(0)$. The tagged source cannot lose any packets when the following conditions are simultaneously met (i) there are k packets in the system in the slot n meaning that the system can accommodate at most $(K - k)$ packets (ii) i, $i = 0, 1, \dots, K - k - 1$ packets arrives from the background source (iii) j, $j = 1, 2, \dots, K - k - i$ arrivals occur from the tagged source. Note that these conditions ensure that $W_B(n) + W_T(n) \leq K - k$. Since no packets are lost in the slot we do not care how packets are arranged in the arrival batch. We obtain

$$f_{L_T}(0, 0) = \frac{\sum_{k=0}^{K-1} \sum_{i=0}^{K-k-1} \sum_{j=1}^{K-k-i} \vec{x}_k D_A(i, j) \vec{e}}{Pr\{W_T(n) \geq 1\}}. \quad (16)$$

where the probability of at least one packet arrival from the tagged source can be found as

$$Pr\{W_T(n) \geq 1\} = \vec{\pi}_T \sum_{i=1}^{\infty} D_T(i) \vec{e}, \quad (17)$$

where $\vec{\pi}_T$ is the steady-state probability vector.

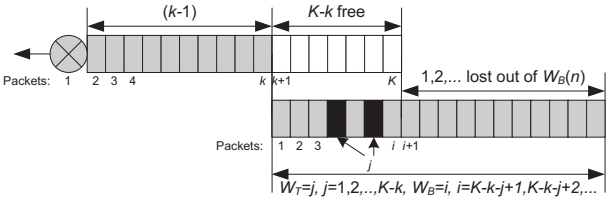

FIGURE 5. All packets from the tagged source are accommodated.

Consider now the case when the tagged source does not lose any packets while losses still occur in a slot, i.e., find the probability $f_{L_T}(0, 1)$. Observe Fig. 5 and note that this happens when the following conditions are simultaneously met (i) there are k packets in the system in the slot n meaning that the system can accommodate at most $(K - k)$ packets (ii) there are j, $j = 1, 2, \dots, K - k$ arrivals from the tagged sources (iii) there are i, $i = K - k - j + 1, K - k - j + 2, \dots$ arrivals from the background source, (iv) all arrivals from the tagged sources are arranged in the arrival batch such that the system accommodates them. Using these conditions, we arrive at

$$f_{L_T}(0, 1) = \frac{\sum_{k=0}^{K-1} \sum_{j=1}^{K-k} \sum_{i=K-k-1}^{\infty} \frac{\vec{x}_{A,k} D_A(i, j) \vec{e}}{[\psi(i, j, K, k, i)]^{-1}}}{Pr\{W_T(n) \geq 1\}}, \quad (18)$$

where $\psi(i, j, K, k, i)$ is the probability that all arriving packets from the tagged source are accommodated by the system given that $W_B(n) = i$ and $W_T(n) = j$ packets arrive from the background and tagged sources, respectively, there are k packets in the system just before arrival of a batch, and the capacity of the system is K. For clarity, we denote this term as $\psi(W_B, W_T, K, k, W_B)$ in what follows.

Consider the term $\psi(W_B, W_T, K, k, W_B)$ and tag an arbitrary packet arriving to the system. Since both arrival processes are of the same priority place occupied by this packet in the arriving batch is distributed uniformly over the size of a batch, i.e., the probability that this packet is at the ith place is given by $1/(W_B + W_T)$. Thus, we can find $\psi(W_B, W_T, K, k, W_B)$ as the ratio of the number of cases favoring the loss of 0 packets from the tagged source to all possible number of cases. Observe Fig. 5 and notice that for the tagged process to not lose a packet in a slot, all its packets need to be at the first $(K-k)$ positions in the arriving batch. This fact implies that only $(K - k - W_T)$ positions are available for arrivals from the background source. Denoting $C_n^k = \binom{n}{k}$ we observe that these arrivals can be arranged using $C_{W_B}^{K-k-W_T}$ ways giving the number of cases favoring no losses from the tagged source. The overall number of ways how $(K - k)$ places can be occupied by arrivals from both processes is $C_{W_B+W_T}^{K-k}$. We have

$$\psi(W_B, W_T, K, k, W_T) = \frac{C_{W_B}^{K-k-W_T}}{C_{W_B+W_T}^{K-k}}. \quad (19)$$

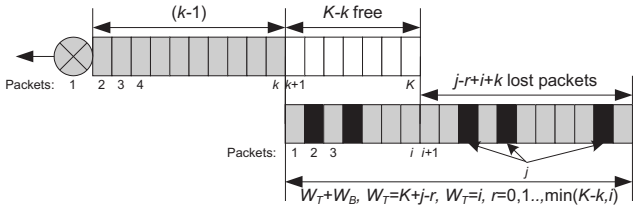

FIGURE 6. Loss of j packets arriving from the tagged source.

Substituting (19) and (17) in (18), (17) in (16), and further summing up (18) and (16) we get $f_{L_T}(0)$.

To obtain the probability that there are j, $j = 1, 2, \ldots$, lost packets from the tagged source in a slot, in addition to placement of packets in the arriving batch we have to take into account the number of packets in the system just before a batch arrival. Also recall that the only component in (15) contributing to $f_{L_T}(i), i = 1, 2, \ldots$ is $f_{L_T}(i, 1)$. Firstly, consider the case when there are no packets in the system in the slot n ($Y_Q(n) = 0$) and the tagged process losses one or more packet. This can only happen when $W_B(n) + W_k(n) > K$. The tagged source losses j packets when the following conditions are simultaneously met (i) i packets arrive from the background source, (ii) at least $(K - k + j)$ packets arrive from the tagged source, and (iii) j packets are not accepted in the system. These conditions are illustrated in Fig. 6, where the case of non-zero packets in the system in the slot n is shown. Taking into account these conditions over all possible transitions of the underlying Markov chain of the superposed arrival process with i, $i = 0, 1, \ldots$ arrivals from the background arrival process and r, $r = 0, 1, \ldots, \min(K, i)$ arrivals from the tagged process, we obtain

$$f_{L_T}(j, 1) = \frac{\sum_{i=0}^{\infty} \sum_{r=0}^{\min(K,i)} \frac{\vec{x}_0 D(i, K + j - r)\vec{e}}{[\psi(i, K + j - r, K, 0, j)]^{-1}}}{Pr\{W_T(n) \geq 1\}}, \quad (20)$$

where $\psi(i, K+j-r, K, 0, j)$ is the probability that j packets from the tagged source are lost given that there are $(K - k)$ places to accommodate arriving packets, and $W_B = i$, $W_T = K + j - r$ packets arrive from the background and the tagged sources, respectively. For clarity of notation we denote this term as $\psi(W_B, W_T, K, k, l_T)$ in what follows.

Extending (20) to the case of k packets in the system just prior a batch arrival, we have

$$f_{L_T}(j, 1) = \quad (21)$$

$$\frac{\sum_{k=0}^{K-1} \sum_{i=0}^{\infty} \sum_{r=0}^{\min(K-k,i)} \frac{\vec{x}_k D(i, K - k + j - r)\vec{e}}{[\psi(i, K - k + j - r, K, k, j)]^{-1}}}{Pr\{W_T(n) \geq 1\}}. \quad (22)$$

Let us now obtain the term $\psi(W_B, W_T, K, k, l_T)$. Note that estimation of this probability is essentially similar to (19). The important difference is that now only $(W_T - l_T)$ packets are accommodated by the system. In order to proceed observe Fig. 6, where arrival of a batch of $(W_B + W_T)$ packets to the queuing system having $(K - k)$ free waiting positions is illustrated. The number of ways how exactly l_T out of W_T packets arriving from the tagged source can be chosen is given by $C_{W_T}^{l_T} = W_T!/l_T!(W_T - l_T)!$. We also have to ensure that we lose exactly $(W_B + W_T - K + k - l_T)$ out of W_B packets from the background source. It can be done using the following number of ways

$$\frac{W_B!}{(W_T + W_B - K + k - l_T)!(W_T - K + k - l_T)!}. \quad (23)$$

Observe now that the product $C_{W_T}^{l_T} C_{W_B}^{W_T+W_B-K+k-l_T}$ gives the number of cases favoring the loss of exactly l_T packets from the tagged source. The overall number of ways to have $(W_B + W_T - K + k)$ lost packets from both tagged and background sources given that $(W_T + W_B)$ packets arrive and the number of free waiting positions is $(K - k)$ is

$$C_{W_B+W_T}^{W_B+W_T-K+k} = \frac{(W_B + W_T)!}{(W_B + W_T - K + k)!(K - k)!}. \quad (24)$$

Thus, the probability that there are exactly l_T lost packets from the tagged source given that there are $(K - k)$ places to accommodate arriving packets and $(W_B + W_T)$ packets arrive from both sources is given by

$$\psi(W_B, W_T, K, k, l_T) = \frac{C_{W_T}^{l_T} C_{W_B}^{W_T+W_B-K+k-l_T}}{C_{W_B+W_T}^{W_B+W_T-K+k}}. \quad (25)$$

Substituting (25), (17) in (21), we obtain the final expression for $f_{L_T}(i)$, $i = 1, 2, \ldots$ Supplementing it with $f_{L_T}(0)$ obtained earlier, we get $f_{L_T}(i)$, $i = 0, 1, \ldots$

V. NUMERICAL ASSESSMENT

In this section, we investigate the packet level performance of mmWave backhauls. First using the results of Section III, we report on essential channel characteristics as a function of system parameters including SNR and capacity. Then, relying on the analysis performed in Section IV, we study loss performance of traffic aggregated from all APs. Finally, we characterize the impact of system parameters on the loss performance of a single AP flow.

The default system parameters used to produce the numerical results are summarized in Table 3. In what follows, whenever a particular parameter is not explicitly specified, its default value is used.

A. CHANNEL CHARACTERISTICS

Before we proceed with reporting on the packet level characteristics of traffic performance over mmWave backhauls we need to understand the response of channel characteristics to transmission system parameters and weather conditions. First, we illustrate the effect of weather conditions on the SNR performance of the channel in Fig. 7, where average conditions from Table 2 are used. Here, snow and fog only slightly affect channel performance while the effect of rain is much more noticeable. Further, foliage provides the drastic

TABLE 3. Default system parameters.

Parameter	Value
Emitted power	2 W
Carrier frequency	28 GHz
Bandwidth	1 GHz
Transmit side antenna array	64×64
Receive side antenna array	64×64
Propagation exponent for clear weather	2.1
Propagation exponent for rainy weather	2.45
Propagation constant	28935037
SNR threshold	0 dB
IP packet size	1500 bytes
Buffer size	300 packets
Offered load of the tagged source	$0.1\rho_A$ Gbps
Arrival rate of aggregated traffic	1.8 Gbps
Arrival rate of the tagged source	$0.1R_A$ pkts/s
Lag-1 NACF of aggregated traffic	0.0
Lag-1 NACF of the tagged source	0.0

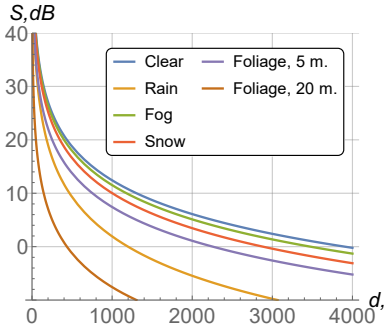

FIGURE 7. Effects of the weather conditions on SNR.

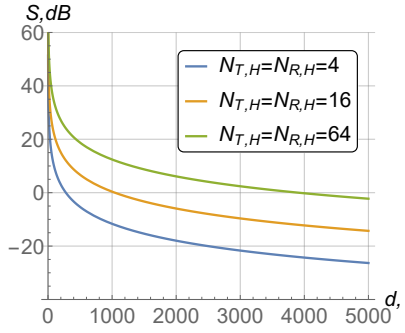

FIGURE 8. SNR as a function of distance.

effect of SNR. In Fig. 7, we illustrate two cases of blockage by foliage. The first case represents sudden blockage of propagation path (caused by, e.g., wind) assuming that signal travels through just 5 meters of foliage. The second case highlights poorly planned backhaul where 20 meters of the propagation path is affected by foliage.

SNR is the channel characteristic affecting communications distance. Fig. 8 shows the SNR as a function of the

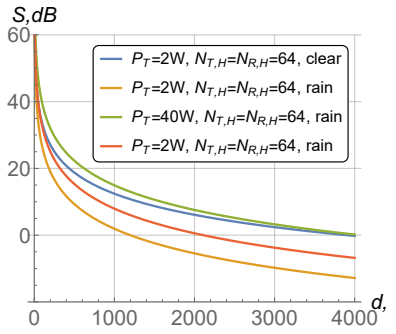

FIGURE 9. SNR as a function of weather conditions.

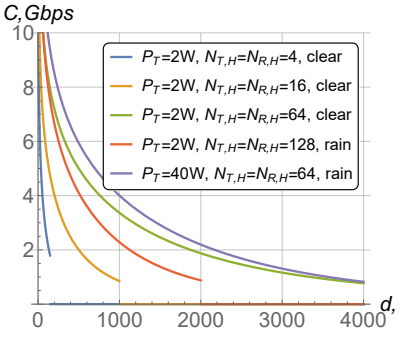

FIGURE 10. Backhaul capacity as a function of system parameters.

communications distance for a number of horizontal transmit and receive antenna array elements. By using the standard emitted power of $2W$ and receiver sensitivity threshold of 0 dB communications distances up to 4000 meters can be achieved with 64 antenna array elements at both sides of a communications link. Recall that 64 horizontal elements also ensure that only insignificant interference is created to adjacent communications systems operating in the same frequency band as the half-power beamwidth (HPBW) is approximated 1.59° [36]. However, as highlighted in Fig. 9 the weather conditions may drastically decrease the achievable communications distance. Notably, the in rain conditions using 2 W of emitted power the effective distance decreases to just 1100 meters.

Regarding communications distance, one needs to use adaptive power control functionality or by increasing the amount of arrays elements forming the transmit and receive antenna radiation patterns. Note that the former approach may not be viable due to governmental regulations on the amount of emitted power. The latter may inherently suffer from as decreasing the HPBW may place additional constraints on beam alignment. In fact, environmental effects such as wind may cause frequent SNR degradation when using extremely narrow beamwidths. Thus, both power adaptation and dynamic antenna arrays are expected to be used in real systems.

To proceed with packet level analysis, we also need to specify the capacity provided by mmWave backhauls. Fig. 10

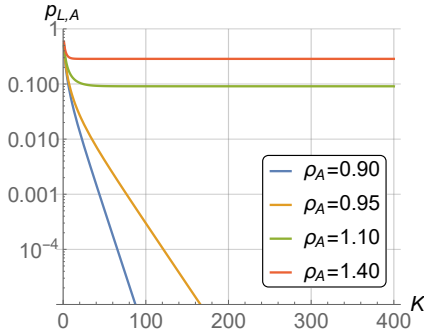

FIGURE 11. Aggregated packet loss probability as a function of buffer size.

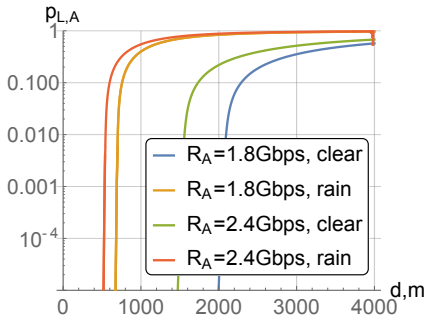

FIGURE 12. Aggregated packet loss probability as a function of distance.

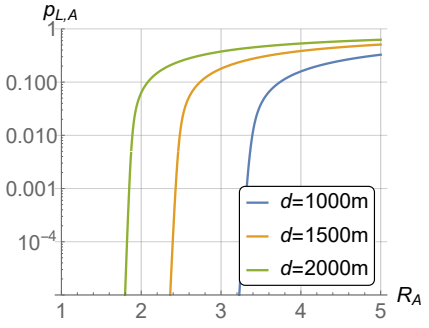

FIGURE 13. Aggregated packet loss probability as a function of arriving traffic rate.

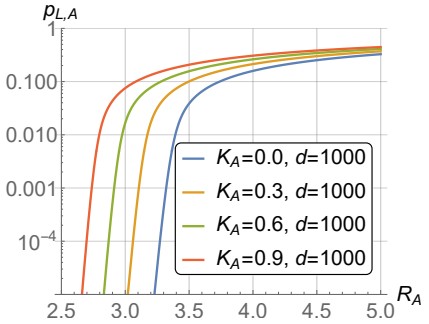

FIGURE 14. Aggregated packet loss probability as a function of lag-1 NACF.

shows the capacity provided in different weather conditions, emitted powers and number of horizontal antenna arrays. For all considered system parameters the capacity decreases exponentially with distance. Both emitted power and antenna arrays provide flexible means to tune the channel capacity. Note that when reaching receiver sensitivity threshold kept at 0dB, the rate is approximately 1 Gbps.

B. AGGREGATED TRAFFIC PERFORMANCE

Let us now proceed characterizing performance of aggregated traffic on mmWave backhauls. The effects of the buffer size and communication distance on packet loss probability are shown in Figs. 11 and 12, where $\rho_A = \lambda_A/\mu_A$ denotes the offered aggregated traffic load. Notably, the effect of the buffer size at these extremely high data rates heavily depends on the value of ρ_A. When $\rho_A < 1$ the packet loss probability is drastically affected by the buffer size. However, even small buffers having less than 200 places for arriving packets (just 300 Kbytes) are efficient enough to keep the packet loss probability lower than 10^{-5}. When $\rho > 1$ the effect of buffer size is negligible. Thus, in what follows, we keep the buffer size at 300 packets.

The effect of backhaul communications distance is shown in Fig. 12 for two values of the arriving traffic rate, R_A, and different weather conditions. Note, that there is a sharp change in the packet loss probability behavior around critical communications distance. This distance corresponds to the point, where the channel rate equals the arriving traffic load, e.g., $\rho_A = 1$. Furthermore, if the system is underutilized, $\rho_A < 1$ almost no packet losses occur while there is a sharp jump to the critical regime when the packet loss probability reaches values higher than 0.1. These conclusions apply to all considered weather conditions.

The effects of arriving traffic rate, R_A for several communications distances, d, and lag-1 NACF values, K_A are illustrated in Figs. 13 and 14. Observe that the higher autocorrelation leads to higher packet loss probability, e.g., for $R_A = 3$ Gbps, $K_A = 0.3$ we have $p_{L,A} \approx 10^{-5}$ while for the same value of the arriving traffic rate and $K_A = 0.6$ the associated packet loss probability is higher than 0.01. This behavior is explained by the specifics induced by the autocorrelation to the arriving stream of packets. Particularly, the higher values of K_A leads to more pronounced "waves" in stochastic traffic behavior. Thus, for the same traffic rate more packets are lost, and the buffer cannot effectively conceal this effect. It is interesting to note by comparing the illustrated data, that the effect of autocorrelation in the arriving traffic stream is equivalent to the change of the backhaul communications distance. For considered system parameters, the increase in the lag-1 NACF value by 0.3 roughly corresponds to the increase in the distance between communicating entities by approximately 100 meters.

C. PER-SOURCE PERFORMANCE

Having observed the importance of aggregated traffic autocorrelation, we now assess whether the autocorrelations of

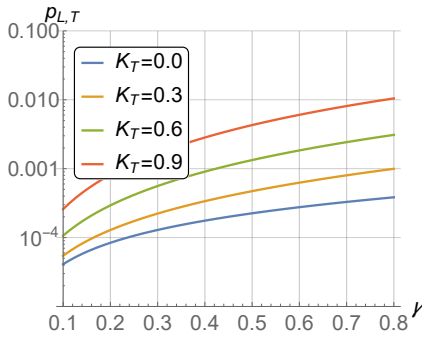

FIGURE 15. Tagged source packet loss probability as a function of lag-1 NACF of tagged source.

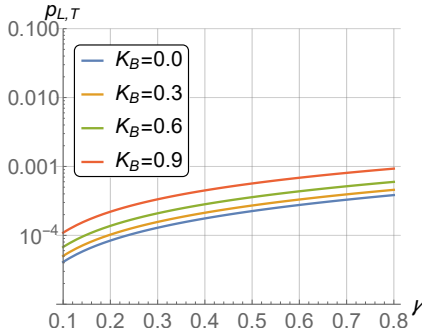

FIGURE 16. Tagged source packet loss probability as a function of lag-1 NACF of background source.

tagged traffic source (e.g., aggregated traffic patterns from a single AP) and background traffic affects the associated packet loss probability. To perform fair comparison and visualize the effect of autocorrelations for different load fractions of the tagged source in the aggregated stream, we fix the communications distance to $d = 1000$ meters, arrival rate of the aggregated traffic to 3.3 Gbps and use γ to represent the load fraction of tagged source, i.e., $R_T = \gamma R_A$.

Figs. 15 and 16 illustrate the effect of autocorrelations of the tagged and background traffic on the packet loss probability of the tagged traffic. According to Fig. 15, the packet loss probability $p_{L,A}$ depends on both the lag-1 NACF value of the tagged traffic and the fraction γ of the tagged traffic. Expectedly, the higher the fraction γ, the higher the difference between curves corresponding to the same value of K_T. For a fixed value of γ, the increase in the packet loss probability is not linear. Notably, the increase caused by changing K_A from 0 to 0.3 is less profound compared to the increase from 0.6 to 0.9. Overall, the autocorrelation results in the adverse effect on the packet loss probability of the tagged traffic.

The effect of the correlation in the background traffic is less profound in the magnitude compared to the effect of correlation in the tagged traffic as evident from Fig. 15. Still, the same trends remain valid. Mainly, the packet loss probability of the tagged source also depends on the load fraction of the tagged source in the traffic aggregate and the trend is qualitatively similar to the effect of the load fraction of the tagged source. Furthermore, for a fixed value of γ, the effect becomes more profound for higher values of K_B.

VI. CONCLUSIONS

The use of mmWave technology for backhaul links is nowadays considered as one of the options for cost-efficient connectivity of remote 3GPP NR APs. In this paper, we have developed a packet level performance evaluation model for mmWave backhaul links that capture the specifics of system design and propagation environment as well as per-AP and aggregated traffic dynamics simultaneously.

Using the developed model, we have revealed that the presence of autocorrelation in the aggregated traffic may severely affect the associated packet loss probability. The effect of autocorrelation is similar to increasing the backhaul communications distance and can be compensated by improving the backhaul rate by either increasing the amount of emitted power or increasing the number of antenna array elements forming the sensitivity or radiation patterns. Analyzing the effect of per-AP traffic and background traffic from other APs on the packet loss probability of the per-AP traffic we have shown that the latter is also affected by autocorrelation. However, the effects of autocorrelation in the per-AP and background traffic is of different magnitudes with the latter producing less profound impact. Furthermore, the effect of autocorrelation of per-AP traffic also depends on the load fraction of this traffic in the whole aggregate.

The developed model can be used for fine-tuning of system parameters of mmWave backhaul dynamically adapting them to changing environmental and traffic conditions. Particularly, knowing the current state of these parameters a network operator may change and transmit and receive side system parameters such that the aggregated and per-AP traffic packet loss probabilities are kept at the acceptable level.

REFERENCES

[1] S.-Y. Lien, S.-L. Shieh, Y. Huang, B. Su, Y.-L. Hsu, and H.-Y. Wei, "5G New radio: waveform, frame structure, multiple access, and initial access," IEEE Communications Magazine, vol. 55, no. 6, pp. 64–71, 2017.

[2] J. Zhang, Z. Zheng, Y. Zhang, J. Xi, X. Zhao, and G. Gui, "3D MIMO for 5G NR: Several Observations from 32 to Massive 256 Antennas Based on Channel Measurement," IEEE Communications Magazine, vol. 56, no. 3, pp. 62–70, 2018.

[3] RCRWireless News, "Who is standalone 5G NR really for?." https://www.rcrwireless.com/20180212/5g/who-is-standalone-5g-nr-really-for-tag17, 2018.

[4] SDX central, "3GPP Approves First 5G Specification." https://www.sdxcentral.com/articles/news/3gpp-approves-first-5g-specification/2017/12/, 2017.

[5] G. Zhang, T. Q. Quek, M. Kountouris, A. Huang, and H. Shan, "Fundamentals of heterogeneous backhaul design–Analysis and optimization," IEEE Transactions on Communications, vol. 64, no. 2, pp. 876–889, 2016.

[6] A. Ometov, E. Sopin, I. Gudkova, S. Andreev, Y. V. Gaidamaka, and Y. Koucheryavy, "Modeling Unreliable Operation of mmWave-Based Data Sessions in Mission-Critical PPDR Services," IEEE Access, vol. 5, pp. 20536–20544, 2017.

[7] X. Ge, H. Cheng, M. Guizani, and T. Han, "5G wireless backhaul networks: challenges and research advances," IEEE Network, vol. 28, no. 6, pp. 6–11, 2014.

[8] 3GPP, "TS 38.874,NR; Study on integrated access and backhaul, Rel. 15," tech. rep., Jan. 2018.

[9] Z. Pi, J. Choi, and R. Heath, "Millimeter-wave gigabit broadband evolution toward 5G: fixed access and backhaul," IEEE Communications Magazine, vol. 54, no. 4, pp. 138–144, 2016.

[10] J. Du, E. Onaran, D. Chizhik, S. Venkatesan, and R. A. Valenzuela, "Gbps User Rates Using mmWave Relayed Backhaul With High-Gain Antennas," IEEE Journal on Selected Areas in Communications, vol. 35, no. 6, pp. 1363–1372, 2017.

[11] U. Habiba, H. Tabassum, and E. Hossain, "Backhauling 5G Small Cells with Massive-MIMO-Enabled mmWave Communication," Backhauling Fronthauling for Future Wireless Systems, p. 29, 2016.

[12] O. Galinina et. al., "Capturing spatial randomness of heterogeneous cellular/WLAN deployments with dynamic traffic," IEEE Journal on Selected Areas in Communications, vol. 32, no. 6, pp. 1083–1099, 2014.

[13] Y. Niu, C. Gao, Y. Li, L. Su, D. Jin, Y. Zhu, and D. O. Wu, "Energy-efficient scheduling for mmWave backhauling of small cells in heterogeneous cellular networks," IEEE Transactions on Vehicular Technology, vol. 66, no. 3, pp. 2674–2687, 2017.

[14] M. N. Kulkarni, J. G. Andrews, and A. Ghosh, "Performance of Dynamic and Static TDD in Self-Backhauled Millimeter Wave Cellular Networks," IEEE Transactions on Wireless Communications, vol. 16, no. 10, pp. 6460–6478, 2017.

[15] A.-A. A. Boulogeorgos, A. Alexiou, T. Merkle, C. Schubert, R. Elschner, A. Katsiotis, P. Stavrianos, D. Kritharidis, P.-K. Chartsias, J. Kokkoniemi, et al., "Terahertz Technologies to Deliver Optical Network Quality of Experience in Wireless Systems Beyond 5G," arXiv preprint arXiv:1803.09060, 2018.

[16] S. Mumtaz, J. M. Jornet, J. Aulin, W. H. Gerstacker, X. Dong, and B. Ai, "Terahertz communication for vehicular networks," IEEE Transactions on Vehicular Technology, vol. 66, no. 7, pp. 5617–5625, 2017.

[17] F. Beritelli, A. Lombardo, S. Palazzo, and G. Schembra, "Performance analysis of an ATM multiplexer loaded with VBR traffic generated by multimode speech coders," IEEE Journal on Selected Areas in Communications, vol. 17, no. 1, pp. 63–81, 1999.

[18] S. Wittevrongel and H. Bruneel, "Per-source mean cell delay and mean buffer contents in ATM queues," Electronics Letters, vol. 33, no. 6, pp. 461–462, 1997.

[19] D. Moltchanov, Y. Koucheryavy, and J. Harju, "Superposed and per-process analysis in $\sum$D-BMAP/D/1/K queuing system," Proc. of HET-NET, p. 42, 2003.

[20] D. Fiems, S. De Vuyst, and H. Bruneel, "Flow loss characteristics in the presence of correlated background traffic," in Proc. of Fifth International Conference on Information Technology: New Generations, pp. 1059–1064, IEEE, 2008.

[21] G. Dán, V. Fodor, and G. Karlsson, "On the effects of the packet size distribution on FEC performance," Computer Networks, vol. 50, no. 8, pp. 1104–1129, 2006.

[22] G. Dán, V. Fodor, and G. Karlsson, "On the effects of the packet size distribution on the packet loss process," Telecommunication Systems, vol. 32, no. 1, pp. 31–53, 2006.

[23] 3GPP, "NR: physical channels and modulation (Release 15)," 3GPP TR 38.211 V15.1.0, Dec. 2017.

[24] 3GPP, "Study on channel model for frequencies from 0.5 to 100 GHz (Release 14)," 3GPP TR 38.901 V14.1.1, July 2017.

[25] D. Solomitckii, V. Semkin, R. Naderpour, A. Ometov, and S. Andreev, "Comparative evaluation of radio propagation properties at 15 GHz and 60 GHz frequencies," in Proc. of 9th International Congress on Ultra Modern Telecommunications and Control Systems and Workshops (ICUMT), pp. 91–95, IEEE, 2017.

[26] G. Brooker, R. Hennessey, C. Lobsey, M. Bishop, and E. Widzyk-Capehart, "Seeing through dust and water vapor: Millimeter wave radar sensors for mining applications," Journal of Field Robotics, vol. 24, no. 7, pp. 527–557, 2007.

[27] S. Sun, G. R. MacCartney, and T. S. Rappaport, "A novel millimeter-wave channel simulator and applications for 5G wireless communications," in Proc. of International Conference on Communications (ICC), pp. 1–7, IEEE, 2017.

[28] A. Ghosh, T. A. Thomas, M. C. Cudak, R. Ratasuk, P. Moorut, F. W. Vook, T. S. Rappaport, G. R. MacCartney, S. Sun, and S. Nie, "Millimeter-wave enhanced local area systems: A high-data-rate approach for future wireless networks," IEEE Journal on Selected Areas in Communications, vol. 32, no. 6, pp. 1152–1163, 2014.

[29] F. Khan and Z. Pi, "mmWave mobile broadband (MMB): Unleashing the 3–300GHz spectrum," in Proc. of 34th Sarnoff Symposium, pp. 1–6, IEEE, 2011.

[30] T. L. Frey, "The Effects of the Atmosphere and Weather on the Performance of a mm-Wave Communication Link," Applied Microwave and Wireless, vol. 11, pp. 76–81, 1999.

[31] H. J. Liebe, T. Manabe, and G. A. Hufford, "Millimeter-wave attenuation and delay rates due to fog/cloud conditions," IEEE Transactions on Antennas and Propagation, vol. 37, no. 12, pp. 1617–1612, 1989.

[32] A. Foessel, S. Chheda, and D. Apostolopoulos, "Short-range millimeter-wave radar perception in a polar environment," 1999.

[33] A. Y. Nashashibi, K. Sarabandi, S. Oveisgharan, M. C. Dobson, W. S. Walker, and E. Burke, "Millimeter-wave measurements of foliage attenuation and ground reflectivity of tree stands at nadir incidence," IEEE Transactions on Antennas and Propagation, vol. 52, no. 5, pp. 1211–1222, 2004.

[34] F. K. Schwering, E. J. Violette, and R. H. Espeland, "Millimeter-wave propagation in vegetation: Experiments and theory," IEEE Transactions on Geoscience and Remote Sensing, vol. 26, no. 3, pp. 355–367, 1988.

[35] V. Petrov, M. Komarov, D. Moltchanov, J. M. Jornet, and Y. Koucheryavy, "Interference and SINR in Millimeter Wave and Terahertz Communication Systems With Blocking and Directional Antennas," IEEE Transactions on Wireless Communications, vol. 16, no. 3, pp. 1791–1808, 2017.

[36] A. B. Constantine et al., "Antenna theory: analysis and design," Microstrip Antennas (third edition), John Wiley & Sons, 2005.

[37] C. Blondia, "A discrete-time batch Markovian arrival process as BISDN traffic model," Belgian J. Operations Research, Statistics and Computer Science, vol. 32, pp. 3–23, 1993.

[38] S. K. Bose, An introduction to queueing systems. Springer Science & Business Media, 2013.

[39] H. Takagi, Queuing analysis: discrete-time systems. North Holland, 1993.

[40] N. Akar, N. C. Oguz, and K. Sohraby, "Matrix-geometric solutions of m/g/1-type markov chains: a unifying generalized state-space approach," IEEE Journal on Selected Areas in Communications, vol. 16, no. 5, pp. 626–639, 1998.

[41] B. Meini, "Fast algorithms for the numerical solution of structured markov chains," 1998.

[42] L. Gemignani, "Efficient and stable solution of structured Hessenberg linear systems arising from difference equations," Numerical linear algebra with applications, vol. 7, no. 5, pp. 319–335, 2000.

[43] N. K. Kim, S. H. Chang, and K. C. Chae, "On the relationships among queue lengths at arrival, departure, and random epochs in the discrete-time queue with D-BMAP arrivals," Operations Research Letters, vol. 30, no. 1, pp. 25–32, 2002.